

# Accepted Manuscript

New insights into the binding mode of pyridine-3-carboxamide inhibitors of *E. coli* DNA gyrase

Sarah Narramore, Clare E.M. Stevenson, Anthony Maxwell, David M. Lawson, Colin W.G. Fishwick

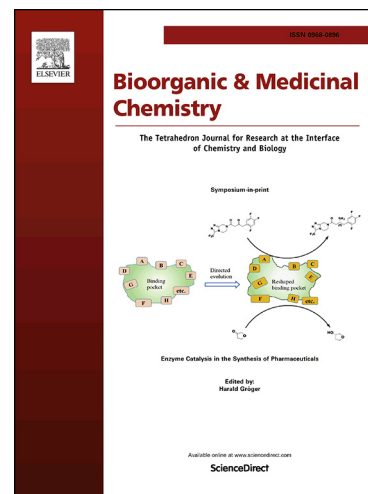
PII: S0968-0896(19)30414-6  
DOI: <https://doi.org/10.1016/j.bmc.2019.06.015>  
Reference: BMC 14952

To appear in: *Bioorganic & Medicinal Chemistry*

Received Date: 26 March 2019  
Revised Date: 24 May 2019  
Accepted Date: 6 June 2019

Please cite this article as: Narramore, S., Stevenson, C.E.M., Maxwell, A., Lawson, D.M., Fishwick, C.W.G., New insights into the binding mode of pyridine-3-carboxamide inhibitors of *E. coli* DNA gyrase, *Bioorganic & Medicinal Chemistry* (2019), doi: <https://doi.org/10.1016/j.bmc.2019.06.015>

This is a PDF file of an unedited manuscript that has been accepted for publication. As a service to our customers we are providing this early version of the manuscript. The manuscript will undergo copyediting, typesetting, and review of the resulting proof before it is published in its final form. Please note that during the production process errors may be discovered which could affect the content, and all legal disclaimers that apply to the journal pertain.



**New insights into the binding mode of pyridine-3-carboxamide inhibitors of *E. coli* DNA gyrase**

Sarah Narramore,<sup>1</sup> Clare E. M. Stevenson,<sup>2</sup> Anthony Maxwell,<sup>2</sup> David M. Lawson and Colin W.G.

Fishwick\*<sup>1</sup>.

1. School of Chemistry and the Astbury Centre for Structural Molecular Biology, University of Leeds, Leeds LS2 9JT, UK.

2. Department of Biological Chemistry, John Innes Centre, Norwich Research Park, Norwich NR4 7UH, UK

**Abstract**

Previously we have reported on a series of pyridine-3-carboxamide inhibitors of DNA gyrase and DNA topoisomerase IV that were designed using a computational de novo design approach and which showed promising antibacterial properties. Herein we describe the synthesis of additional examples from this series aimed specifically at DNA gyrase, along with crystal structures confirming the predicted mode of binding and *in vitro* ADME data which describe the drug-likeness of these compounds.

**Introduction**

Antibacterial resistance continues to be a growing threat to human health worldwide. The rate of discovery of new antibacterials is far outstripped by the rate at which resistance is spreading, and there remains an urgent need for the development of new antibacterial drugs<sup>1</sup>. Of particular concern is the emergence of bacterial strains that appear to be totally resistant to all current antibacterials. This was recently underlined by the CDC, who reported a case in which a patient in the US was infected with a strain of *Klebsiella pneumoniae* that was resistant to all available antibiotics.<sup>2</sup>

DNA topoisomerases are an essential class of enzymes responsible for maintaining the topological state of DNA (e.g. supercoiling)<sup>3</sup>. The ATP-dependent bacterial type II topoisomerases, DNA gyrase and DNA topoisomerase IV, contribute to the maintenance of the correct level of supercoiling in bacterial DNA. These enzymes are hetero-tetramers, e.g. gyrase consists of two subunits, GyrA and GyrB, which form an A<sub>2</sub>B<sub>2</sub> complex<sup>4</sup>. These enzymes have been well-validated as antibacterial targets as the fluoroquinolone antibiotics act at the DNA-cleavage site of these enzymes. The aminocoumarin antibiotics, including novobiocin, which was used clinically in the 1960's, target the ATP-binding site. Efforts to discover novel inhibitors of the ATP-binding site of these enzymes have been ongoing for more than four decades. However, only two compounds have progressed into the clinic<sup>5</sup>.

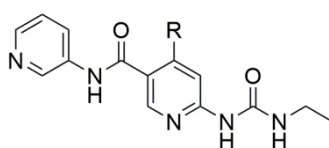
We have previously reported a series of pyridine-3-carboxamide inhibitors of DNA gyrase and topoisomerase IV which displayed antibacterial activity<sup>6</sup>. These compounds, designed to bind to the ATP-binding site within the gyrase using the *de novo* molecular design program SPROUT<sup>7</sup>, were developed into a series possessing promising antibacterial activity. However, the computationally predicted binding mode of these molecules has not been previously validated experimentally and little assessment was made of the potential "drug-likeness" of compounds in this series. We now report the detailed structural characterisation of the binding mode of these inhibitors within bacterial GyrB as well as delineation of a number of key physicochemical parameters of importance in considering their potential for progression into antibacterial drugs.

## Results and discussion

### Biological activity of novel pyridine-2-urea-3-carboxamide (PUC) inhibitors

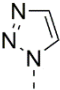
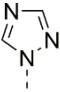
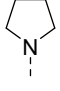
As part of a program designed to expand upon our previously reported studies<sup>6</sup>, a small library of novel PUC inhibitors was synthesised with a view to establishing the best candidates for subsequent co-crystallisation studies with the target enzymes. As with previous examples<sup>6</sup>, the synthetic strategy

was informed by a number of molecular modelling techniques. Putative compounds were initially developed via *de novo* design utilising SPROUT. The most likely inhibitors of *E. coli* GyrB were then identified via docking studies using Glide, with the highest-scoring compounds taken forward for synthesis<sup>9</sup>. Following synthesis of the identified compounds, the inhibitory activity of these compounds, together with their antibacterial activities, was established as described previously<sup>6</sup>. A summary of the biological activities of these compounds are given below (Table 1).



**Table 1.** Biological activity of selected pyridine urea carboxamide compounds. (See Supporting Information).

Compound	R	IC <sub>50</sub> (μM)	MICs (μg/ mL)	
		Ec gyrase	SA	EC
1		0.41	>64	>64
2		0.019	4	>64
3		0.089	>64	>64
4		0.086	64	>64
5		0.037	16	>64
6		0.15	64	>64

7		0.20	n.d.	n.d.
8		0.082	>64	>64
9		0.12	64	>64

Ec gyrase, *E. coli* DNA gyrase ATPase; SA, *S. aureus* ATCC 29213; EC, *E. coli* ATCC 25922.

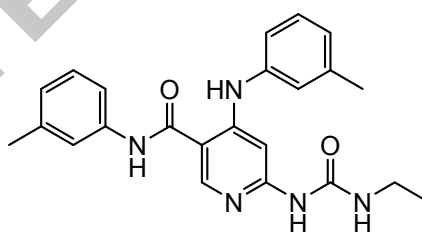
As shown in Table 1, several of these compounds were found to be potent inhibitors of *E. coli* DNA gyrase, particularly compound **2**. However, with regards to antibacterial activity, although compound **2** shows some promise against *S. aureus* (MIC = 4 µg/ml), the rest of the inhibitors were less active and unfortunately, none of the compounds tested showed any activity against the Gram negative organism *E. coli*. This was somewhat disappointing given the encouraging antibacterial activity we had previously established for this class of compounds (e.g. compound **10**, Figure 1)<sup>6</sup>.

Recent work by Hergenrother has correlated specific structural aspects of small molecules with their ability to penetrate into bacterial cells<sup>8</sup>. This work has demonstrated that the presence of a primary amine, along with a relatively flat molecular shape (corresponding to a 'globularity' of 0.25 or lower, where flat molecules such as benzene have a globularity = 0, and spherical molecules like adamantane have globularity = 1 ), together with a limited degree of molecular flexibility (five or fewer rotatable bonds), maximises the likelihood of cell penetration into *E. coli* bacteria. Furthermore, the work has strongly linked these structural features with penetration into the bacteria cell via porins. Applying these analyses (using the online eNTRY properties calculator<sup>7</sup>) to molecules **1** – **10** confirms that, although all molecules have favourably low globularity (values ranging from 0.022 – 0.057), almost all are predicted to poorly enter *E. coli* bacteria, due to either the lack of a primary amine function (molecules **1**, **2**, **4** – **10**), and, in the case of **1**, **2**, and **10**, also having greater than five rotatable bonds. An interesting exception however, is the primary amine-based system **3** which, despite conforming well to all three requirements, lacks inhibitory activity

towards *E. coli* (see Supporting Information). This may indicate that other factors such as the role of bacterial efflux pumps, may be of prime importance in dictating the antibacterial activity for this class of molecules in *E. coli*. Indeed, we had previously reported that, although devoid of antibacterial activity in the presence of wild type *E. coli*, a number of similar pyridine-3-carboxamides showed antibacterial activity (8 – 32 µg/ml) towards *E. coli* lacking an efflux pump<sup>6</sup>.

#### Characterisation of the binding of PUC inhibitors using crystallisation and X-ray diffraction studies

In order to investigate the binding modes of the PUC inhibitors within GyrB, co-crystallisation of a number of the inhibitors with a 24 kDa subunit of the GyrB unit ('GyrB24') of the DNA gyrase enzyme was carried out<sup>9</sup>. The gene for the 24 kDa subunit of GyrB was transformed into a pNIC vector to give a hexahistidine tagged version of the protein. The protein was expressed and purified using a nickel-affinity chromatography and following purification the histidine tag was cleaved. The protein was crystallised in the presence of compounds **2**, **4**, **5** and **10** respectively. We had previously reported that compound **10** (Figure 1) had shown encouraging degrees of biological activity.



**10**

*E. coli* GyrB IC<sub>50</sub> (µM): 0.099

*S. aureus* MIC<sub>50</sub> (µg/mL): 1.0

*E. faecalis* MIC<sub>50</sub> (µg/mL): 0.5

**Figure 1.** Structure and biological activities of previously reported GyrB inhibitor **10**

The crystal structures of GyrB24 with compounds **2**, **4** and **5** bound respectively, were determined to 2.50-, 1.95-, and 1.90-Å resolution respectively (see Supporting Information). An additional crystal structure involving our previously reported inhibitor **10** (Figure 1) was also determined at 2.35- Å resolution. The models each consisted of one monomer of protein in the asymmetric unit with one

molecule of inhibitor bound in the ATP-binding site. The crystal structures confirmed that these inhibitors bind in the ATPase site of the enzyme in an orientation closely resembling that originally designed using SPROUT<sup>6</sup>, and also consistent with the binding pose predicted by using a computational docking utilising the Glide programme<sup>10</sup> (Figure 2).

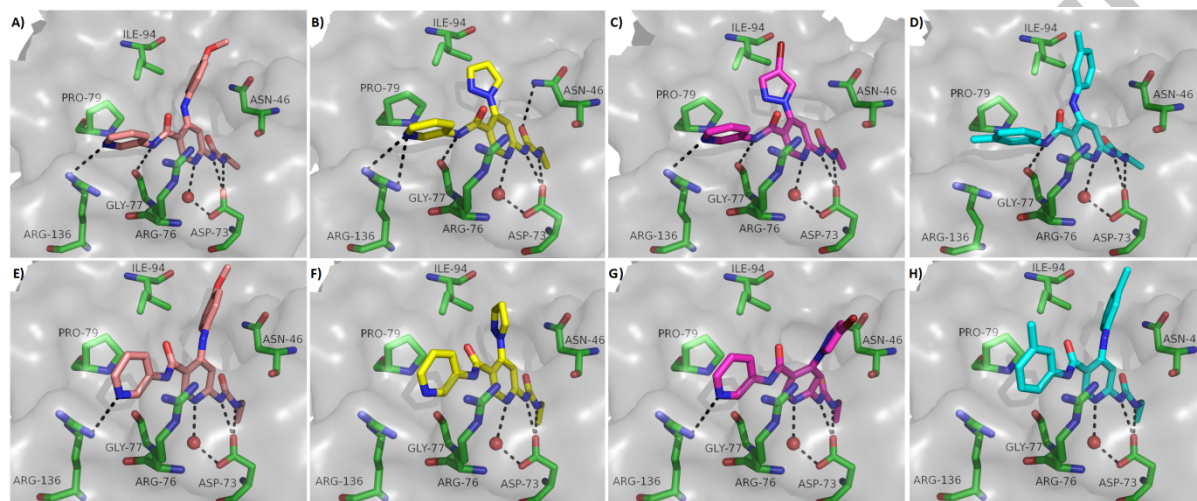


**Figure 2** Comparison of binding poses of inhibitors predicted using Glide docking in *E. coli* GyrB (bottom row) with X-ray co-crystal structures where the key residues which form interactions with the inhibitors are shown in green and the protein surface in grey (top row). Dashed lines indicate a hydrogen bond where the interatomic distance is  $<3.5$  Å. A) Compound **2** co-crystallised; B) Compound **4** co-crystallised; C) Compound **5** co-crystallised; D) Compound **10** co-crystallised; E) Compound **2** docked; F) Compound **4** docked; G) Compound **5** docked; H) Compound **10** docked.

Inspection of the crystal structures of GyrB containing these inhibitors reveals a number of aspects common to all co-crystal structures. Specifically, as is the case with a number of other known inhibitors which bind at the ATP-binding site of GyrB, a hydrogen bonding network involving Asp-73 and a conserved water molecule in the binding site can be seen. The hydrogen bond donation from the urea moiety and hydrogen bond acceptance from the pyridine rings within the inhibitor molecules closely mirror the poses predicted via the computational modelling studies.

The co-crystal structures obtained also compare favourably with previous series of GyrB inhibitors; including ethyl urea series such as those generated by Panchaud *et al* in 2017 (Figure 3)<sup>11</sup>. The

binding mode of the compounds presented in this work is highly conserved with these previous examples – featuring the same crucial interactions between the urea/pyridine moiety, Asp-73, and the same conserved water molecule. This observation corresponds well with the similar GyrB  $IC_{50}$  values for these two example compounds of 0.125  $\mu$ M and 0.03  $\mu$ M respectively – with the slightly higher potency of compound **2** explained via the introduction of hydrogen-bond interactions between the terminal pyridine and Arg-136. The overall structure of the ATP binding site is highly conserved between the Panchaud *et al* example and our newly generated structures, with the residues occupying near-identical areas and orientations.

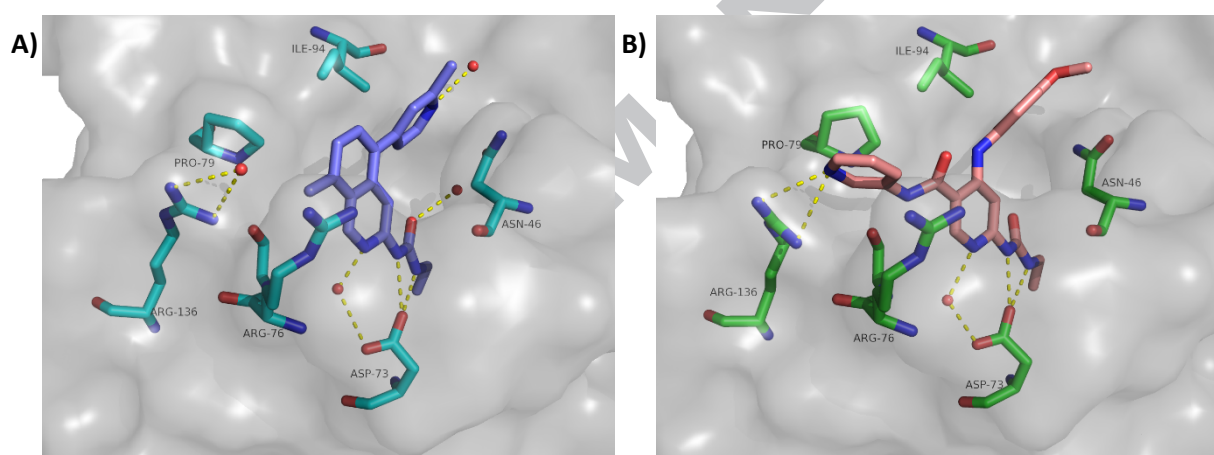


**Figure 3** Comparison of a previous *E. coli* GyrB X-ray co-crystal structure (PDBID: 5MMN)<sup>11</sup> with our newly-generated X-ray co-crystal structures. A) The co-crystal structure of 1-ethyl-3-[8-methyl-5-(2-methyl-pyridin-4-yl)-isoquinolin-3-yl]-urea with *E. coli* GyrB obtained by Panchaud *et al* in 2017<sup>11</sup>. B) The co-crystal structure of compound **2** with *E. coli* GyrB.

#### ADME Profiling of PUC inhibitors.

Compound **2**, **3**, **4** and **10** were profiled for their *in vitro* ADME properties; the results are shown in Table 2.

**Table 2.** ADME properties of selected PUC inhibitors.



Compound	Aqueous solubility <sup>a</sup> ( $\mu$ M)	Human Plasma protein binding <sup>a</sup> (%)	Caco-2 permeability A-B <sup>a</sup> ( $P_{app} \times 10^6 / \text{cm} \cdot \text{s}^{-1}$ )	Caco-2 efflux ratio <sup>a</sup> $P_{app}(\text{B-A}) / P_{app}(\text{A-B})$	Human liver microsome $t_{1/2}$ <sup>a</sup> (mins)	Mouse liver microsome $t_{1/2}$ <sup>a</sup> (mins)
<b>2</b>	2.4	97.2	11.83	2.82	20	n/d
<b>3</b>	88.5	50.2	4.02	2.78	290	n/d
<b>4</b>	32.6	90.5	1.23	30.8	128	24
<b>10</b>	4.26	99.9	<2.67 <sup>b</sup>	n/a	46	58

a) assays carried out by Shanghai ChemPartner Ltd. b)  $P_{app}$  values were expressed as "<" than the values that were calculated using the minimum concentration of the standards for receiver sides as the concentration in the receivers was below the quantitation limit.

A review of the data in Table 2 reveals some interesting trends in physicochemical properties within the PUC series of inhibitors. The aqueous solubility of compounds **2**, **4** and **10** was found to be rather low suggesting that these specific structures within the PUC series would be unattractive in terms of development as orally bioavailable drug leads. This is mirrored by the high levels of plasma protein binding seen for these compounds. However, compound **3**, containing an aminopyrrolidine substituent, showed a much higher aqueous solubility and correspondingly lower plasma protein binding.

An estimate of the ability of these compounds to cross biological membranes was also carried out using the Caco-2 permeability assay, which uses a human intestinal cell line to model absorption of a compound from the gut<sup>12</sup>. The rate of transfer of compound is measured in both directions across the cell membrane. The rate of transfer in the A-B direction (mimicking transfer from the gut to the blood) and the efflux ratio (an indicator that a compound will fail to be absorbed due to efflux) are given in Table 2. Compounds **2** and **3** performed the best in this assay showing a moderate permeability and lower efflux ratios than the other compounds. Compound **4** displayed low

permeability and a high efflux ratio. Full data could not be obtained for compound **10**, due to solubility preventing reliable measurements to be made.

Microsomal stability assays were also carried out in mice liver microsomes and human liver microsomes respectively. In the human liver microsome assay, the most stable compound tested was compound **3**, which had a half-life ( $t_{1/2}$ ) of 290 minutes. Compounds **2** and **10** were the least metabolically stable. This suggests that the aryl amine groups are more sensitive metabolically than the pyrazole-based moieties. Addition of functional groups to the aniline rings which are known to slow metabolism, such as  $\text{CF}_3$  could increase the metabolic half-life of these compounds<sup>13</sup>.

Finally, we also investigated the selectivity of this class of inhibitor for bacterial gyrase versus inhibition of human topoisomerase II. Four representative compounds (**2**, **3**, **4**, and **5**) were tested for activity against human topoisomerase II $\alpha$ . In all cases, we found little or no inhibition of the human enzyme with compound concentrations up to 100  $\mu\text{M}$ , suggesting that the human enzyme is at least 1000-fold less sensitive than bacterial gyrase (data not shown).

## Conclusions

In this study, protein X-ray crystallography has been used to explore the detailed mode of binding of the pyridine carboxamide class of antibacterial agents, to their bacterial DNA gyrase target. These studies reveal that the binding mode of these inhibitors closely corresponds to that predicted via the structure-based design approach used in their conception, in particular, confirming the importance of an exquisite network of H-bonds involving all three nitrogen atoms shared between the urea and pyridine units within the inhibitors, a bound water molecule, and serine and aspartate amino acids derived from the protein.

A preliminary analysis of the development potential of these compounds for use as antibacterials via measurement of a range of *in vitro* ADMET parameters reveals that, whilst some of the compounds possess a rather low degree of aqueous solubility, with a corresponding increase in plasma-protein

binding, solubility can be increased to encouraging levels via suitable structural alteration, as underlined by compound **3**, which also shows promising levels of metabolic stability. However, the weak antimicrobial activity measured for this compound, despite the good affinity it displays for GyrB, underlines one of the key challenges of target-based antimicrobial drug design in terms of producing compounds with high target affinity and selectivity, but which also possess the right blend of physicochemical properties to allow passage into- and retention within- the bacterial cell, a requirement that is particularly challenging for entry into Gram negative organisms.

## Experimental Section

The [Supporting Information](#) contains a complete general Experimental Section, including all procedures and equipment used. Chemicals were from commonly used suppliers (Aldrich, Acros, and Alfa Aesar) and used without purification. The purities of compounds submitted for screening were  $\geq 95\%$  as determined by UV analysis of liquid chromatography (HPLC) chromatograms at 254 nm.

**Representative Synthesis for Compound 1.** *Synthesis of 4-chloro-6-[(ethylcarbamoyl)amino]-N-(pyridin-3-yl)pyridine-3-carboxamide.* Ethyl 4-chloro-6-(3-ethylureido)nicotinate<sup>6</sup> (700 mg, 2.57 mmol) was suspended in NaOH (2 M, 30 ml) and heated to 80°C for 16 hours. The reaction mixture was then cooled to 0°C and acidified to pH 4 by dropwise addition of cHCl. The resulting precipitate was collected using filtration, washed with water and dried under air to afford the carboxylic acid intermediate (516 mg, 2.12 mmol, 83%) as pale-yellow microcrystals. The carboxylic acid (516 mg, 1.12 mmol) and 3-amino pyridine (439 mg, 4.70 mmol) were dissolved in EtOAc (5 ml), and pyridine (0.5 ml) and T3P (5 ml, 58.2 mmol, 50% solution in EtOAc) were added. The reaction mixture was stirred at room temperature for 18 hours and then basified to pH 10 by addition of aqueous NaOH (2 M). The mixture was then stirred for 20 minutes and the product collected by filtration to afford the product (230 mg, 0.72 mmol, 34%) as pale orange microcrystals, m.p. 210.4-215.6 °C;  $R_f$  0.24 (1:1 EtOAc–Pet);  $\delta_H$  (300 MHz, DMSO- $d_6$ ) 10.74 (s, 1 H, 4-NH), 9.57 (s, 1 H, 6-NHCONHCH<sub>2</sub>CH<sub>3</sub>), 8.84 (d,  $J$  2.2 Hz, 1 H, 3-pyridyl 2-H), 8.47 (s, 1 H, 2-H), 8.33 (d, 1 H,  $J$  3.8 Hz, 3-pyridyl 6-H), 8.15 (d,  $J$  8.8 Hz, 1

H, 3-pyridyl 4-H), 7.80 (s, 1 H, 5-H), 7.31-7.50 (m, 2 H, 3-pyridyl 5-H and 6-NHCONHCH<sub>2</sub>CH<sub>3</sub>), 3.18 (qd, *J* 7.2 and 5.5 Hz, 2 H, 6-NHCONHCH<sub>2</sub>CH<sub>3</sub>), 1.09 (t, *J* 7.2 Hz, 3 H, 6-NHCONHCH<sub>2</sub>CH<sub>3</sub>);  $\delta_c$  (125 MHz DMSO-*d*<sub>6</sub>) 163.1 (3-CONH), 155.0 (6-C), 154.0 (6-NHCONHCH<sub>2</sub>CH<sub>3</sub>), 148.0 (2-C), 144.8 (3-pyridyl 6-C), 141.6 (3-pyridyl 2-C), 141.2 (3-pyridyl 3-C), 135.5 (4-C), 126.5 (3-pyridyl 4-C), 124.8 (3-C), 123.7 (3-pyridyl 5-C), 111.2 (5-C), 33.9 (6-NHCONHCH<sub>2</sub>CH<sub>3</sub>), 15.2 (6-NHCONHCH<sub>2</sub>CH<sub>3</sub>);  $\nu_{\max}$  / cm<sup>-1</sup> (solid) 3179, 1669, 1548; *m/z* (ES<sup>+</sup>) found MH<sup>+</sup> 320.0912 C<sub>14</sub>H<sub>14</sub>ClN<sub>5</sub>O<sub>2</sub> *MH* requires 320.0909; HPLC RT = 0.99 mins.

Synthesis of 6-[(ethylcarbamoyl)amino]-4-[(2-hydroxyphenyl)amino]-N-(pyridin-3-yl)pyridine-3-carboxamide. 4-Chloro-6-[(ethylcarbamoyl)amino]-N-(pyridin-3-yl)pyridine-3-carboxamide (30 mg, 0.09 mmol) and 2-hydroxyaniline (30 mg, 0.09 mmol) were dissolved in ethanol (2 ml) and NEt<sub>3</sub> (5 drops) was added. The reaction was heated to 80°C for 3 hours. The reaction was then allowed to cool to room temperature and the solvent removed *in vacuo*. The resulting off white residue was taken up in EtOAc (10 ml), washed with water (3 × 10 ml) and brine (10 ml), the volume reduced *in vacuo* and the product collected by filtration to afford the product (7.5 mg, 0.191 mmol, 21%) as pale red microcrystals, *R*<sub>f</sub> 0.03 (EtOAc);  $\delta_H$  (500 MHz, DMSO-*d*<sub>6</sub>) 10.43 (br. s., 1 H, 3-CONH), 9.85 (s, 1 H, 6-NHCONHCH<sub>2</sub>CH<sub>3</sub>), 9.77 (s, 1 H, 4-NH), 9.14 (s, 1 H, 4-phenyl 6-H), 8.88 (s, 1 H, 3-pyridyl 2-H), 8.61 (s, 1 H, 2-H), 8.33 (d, 1 H, *J* 4.6 Hz, 3-pyridyl 6-H), 8.14 (d, *J* 7.8 Hz, 1 H, 3-pyridyl 4-H), 8.00 (br. s., 1 H, 4-phenyl OH), 7.41 (dd, *J* 8.5, 4.8 Hz, 1 H, 3-pyridyl 5-H), 7.32 (d, *J* 7.8 Hz, 1 H, 4-phenyl 3-H), 7.23 (s, 1 H, 5-H), 6.91 - 7.03 (m overlapping, 2 H, 4-phenyl 4-H and 5-H), 6.86 (t, *J* 6.9 Hz, 1 H, 6-NHCONHCH<sub>2</sub>CH<sub>3</sub>), 3.17 (qd, *J* 7.1, 6.9 Hz, 2 H, 6-NHCONHCH<sub>2</sub>CH<sub>3</sub>), 1.09 (t, *J* 7.1 Hz, 3 H, 6-NHCONHCH<sub>2</sub>CH<sub>3</sub>);  $\delta_c$  (500 MHz, DMSO-*d*<sub>6</sub>) 166.9 (3-CONH), 155.9 (4-phenyl 2-C), 154.4 (6-C), 152.1 (4-C), 149.6 (6-NHCONHCH<sub>2</sub>CH<sub>3</sub>), 149.0 (5-C), 144.6 (3-pyridyl 2-C), 142.2 (3-pyridyl 6-C), 127.7 (3-pyridyl 4-C), 126.5 (4-phenyl 1-C), 124.7 (4-phenyl 4-C), 123.5 (3-pyridyl 5-C), 122.1 (4-phenyl 5-C), 119.2 (4-phenyl 6-C), 115.8 (4-phenyl 3-C), 108.0 (3-C), 92.0 (2-C), 33.8 (6-NHCONHCH<sub>2</sub>CH<sub>3</sub>), 15.3 (6-NHCONHCH<sub>2</sub>CH<sub>3</sub>);  $\nu_{\max}$  / cm<sup>-1</sup> (solid) 2969, 2811, 1698, 1642, 1543, 1517; *m/z* (ESI<sup>+</sup>) found MH<sup>+</sup> 393.1673, C<sub>20</sub>H<sub>20</sub>N<sub>6</sub>O<sub>3</sub> *MH* requires 393.1670; HPLC RT = 1.38 mins.

**Associated Content****Supporting Information**

The Supporting Information is available free of charge on the ScienceDirect Publications website at

DOI:....

Experimental procedures, characterization of intermediates and target compounds, description of protein production and purification, molecular modelling, biological assays, x-ray crystallography.

**Author information****Corresponding Author**

\*Phone: +44 (0) 1133 436510; e-mail: [c.w.g.fishwick@leeds.ac.uk](mailto:c.w.g.fishwick@leeds.ac.uk).

**ORCID**

Colin W. G. Fishwick: [0000-0003-1283-2181](https://orcid.org/0000-0003-1283-2181)

Anthony Maxwell: [0000-0002-5756-6430](https://orcid.org/0000-0002-5756-6430)

**Notes and acknowledgements**

The authors declare no competing financial interest.

The authors declare no competing financial interest.

Crystal data for compounds **2**, **4**, **5**, and **10** have been deposited in the Protein Data Bank with accession codes 6F86, 6F8J, 6F94 and 6F96

The authors thank Alison Howells (Inspiralis Ltd.) for carrying out supercoiling and relaxation assays.

**Abbreviations used**

ADME, absorption distribution metabolism excretion; ATP, adenosine triphosphate; BSA, bovine serum albumin; CaCo-2, human carcinoma colon cell line; CDC, Centers for Disease Control and Prevention; cHCl, concentrated hydrochloric acid; CHCl<sub>3</sub>, chloroform; DCM, dichloromethane; dCTP, deoxycytosine triphosphate; dGTP, deoxyguanosine triphosphate; DMSO, dimethyl sulfoxide; *E. coli*, *Escherichia coli*; EDTA, ethylenediaminetetraacetic acid; GyrA, DNA gyrase subunit A; GyrB, DNA gyrase subunit B; DTT, dithiothreitol; EtOAc, ethyl acetate; HEPES, 4-(2-hydroxyethyl)-1-piperazineethanesulfonic acid; HPLC, high performance liquid chromatography; IC<sub>50</sub>, inhibitory concentration at half maximal; KCl, potassium chloride; MeOH, methanol; MgCl<sub>2</sub>, magnesium chloride; MgSO<sub>4</sub>, magnesium sulphate; MIC, minimum inhibitory concentration; m.p., melting point; NAD<sup>+</sup>, nicotinamide adenine dinucleotide; NADH, nicotinamide adenine dinucleotide reduced form; NaOH, sodium hydroxide; NEB, New England Biolabs; NEt<sub>3</sub>, trimethylamine; NiSO<sub>4</sub>, nickel sulphate; PCR, polymerase chain reaction; PEG, polyethylene glycol; Pet, petroleum ether; RT, room temperature; *S. aureus*, *Staphylococcus aureus*; SDS-PAGE, sodium dodecyl sulfate–polyacrylamide gel electrophoresis; SOC, super optimal broth with catabolite suppression; T3P, propyl phosphonic anhydride; Tris, tris(hydroxymethyl)aminomethane.

## References

1. Piddock, L. J. V. Reflecting on the final report of the O'Neill Review on Antimicrobial Resistance. *The Lancet Infectious Diseases* **16**, 767-768.
2. Chen, L.; Todd, R.; Kiehlbauch, J.; Walters, M.; Kallen, A. Notes from the Field: Pan-Resistant New Delhi Metallo-Beta-Lactamase-Producing *Klebsiella pneumoniae* — Washoe County, Nevada, 2016. *MMWR Morb Mortal Wkly Rep* **2017**, *66*, 33.
3. Schoeffler, A. J.; Berger, J. M. DNA topoisomerases: harnessing and constraining energy to govern chromosome topology. *Quarterly reviews of biophysics* **2008**, *41*, 41-101.
4. Bush, N.; Evans-Roberts, K.; Maxwell, A. DNA Topoisomerases. *EcoSal Plus* **2015**.
5. Bisacchi, G. S.; Manchester, J. I. A New-Class Antibacterial—Almost. Lessons in Drug Discovery and Development: A Critical Analysis of More than 50 Years of Effort toward ATPase Inhibitors of DNA Gyrase and Topoisomerase IV. *ACS Infectious Diseases* **2015**, *1*, 4-41.
6. Yule, I. A.; Czaplewski, L. G.; Pommier, S.; Davies, D. T.; Narramore, S. K.; Fishwick, C. W. G. Pyridine-3-carboxamide-6-yl-ureas as novel inhibitors of bacterial DNA gyrase: Structure based design, synthesis, SAR and antimicrobial activity. *European Journal of Medicinal Chemistry* **2014**, *86*, 31-38.

7. Gillet, V.; Johnson, A. P.; Mata, P.; Sike, S.; Williams, P. SPROUT - a program for structure generation. *Journal of Computer-Aided Molecular Design* **1993**, *7*, 127-153.
8. Richter, M. F.; Drown, B. S.; Riley, A. P.; Garcia, A.; Shirai, T.; Svec, R. L.; Hergenrother, P. J. Predictive Compound Accumulation Rules Yield a Broad-Spectrum Antibiotic. *Nature* **2017**, *545*, 299-304.
9. Lewis, R. J.; Singh, O. M.; Smith, C. V.; Skarzynski, T.; Maxwell, A.; Wonacott, A. J.; Wigley, D. B. The nature of inhibition of DNA gyrase by the coumarins and the cyclothialidines revealed by X-ray crystallography. *The EMBO journal* **1996**, *15*, 1412-20.
10. *Maestro version 10.0*. Schrödinger, LLC, New York, NY: 2014.
11. Panchaud, P.; Bruyère, T.; Blumstein, A.-C.; Bur, D.; Chambovey, A.; Ertel, E. A.; Gude, M.; Hubschwerlen, C.; Jacob, L.; Kimmerlin, T.; Pfeifer, T.; Prade, L.; Seiler, P.; Ritz, D.; Rueedi, G. Discovery and Optimization of Isoquinoline Ethyl Ureas as Antibacterial Agents. *Journal of Medicinal Chemistry* **2017**, *60*, 3755-3775.
12. Sambuy, Y.; Angelis, I.; Ranaldi, G.; Scarino, M. L.; Stamatii, A.; Zucco, F. The Caco-2 cell line as a model of the intestinal barrier: influence of cell and culture-related factors on Caco-2 cell functional characteristics. *Cell Biology and Toxicology* **2005**, *21*, 1-26.
13. Gillis, E. P.; Eastman, K. J.; Hill, M. D.; Donnelly, D. J.; Meanwell, N. A. Applications of Fluorine in Medicinal Chemistry. *Journal of Medicinal Chemistry* **2015**, *58*, 8315-8359.

#### Table of Contents graphic

